

RESEARCH ARTICLE

SIMP-ALL: A generalized SIMP method based on the topological derivative concept

A. Ferrer^{1,2} 

¹Centre de Mathématiques Appliquées,
École Polytechnique, Université
Paris-Saclay, Palaiseau, France

²Centre Internacional de Mètodes
Numèrics en Enginyeria (CIMNE),
Campus Nord UPC, Barcelona, Spain

Correspondence

A. Ferrer, Centre de Mathématiques
Appliquées, École Polytechnique,
Université Paris-Saclay, 91128 Palaiseau,
France; or Centre Internacional de
Mètodes Numèrics en Enginyeria
(CIMNE), Campus Nord UPC, Edifici C-1,
c/Jordi Girona 1-3, 08034 Barcelona, Spain.
Email: aferrer@cimne.upc.edu

Funding information

European Union's Horizon 2020 research
and innovation programme, Grant/Award
Number: 712949; Agency for Business
Competitiveness of the Government of
Catalonia

Summary

Topology optimization has emerged in the last years as a promising research field with a wide range of applications. One of the most successful approaches, the SIMP method, is based on regularizing the problem and proposing a penalization interpolation function. In this work, we propose an alternative interpolation function, the SIMP-ALL method that is based on the topological derivative concept. First, we show the strong relation in plane linear elasticity between the Hashin-Shtrikman (H-S) bounds and the topological derivative, providing a new interpretation of the last one. Then, we show that the SIMP-ALL interpolation remains always in between the H-S bounds regardless the materials to be interpolated. This result allows us to interpret intermediate values as real microstructures. Finally, we verify numerically this result and we show the convenience of the proposed SIMP-ALL interpolation for obtaining auto-penalized optimal design in a wider range of cases. A MATLAB code of the SIMP-ALL interpolation function is also provided.

KEYWORDS

Hashin-Shtrikman bounds, SIMP, topological derivative, topology optimization

1 | INTRODUCTION

In the recent years, topology optimization has become a research field by itself, not only because it arouses interest on the scientific community but also because it provides successful solutions to industrial problems.¹ Traditionally, topology optimization seeks to design light-weight structural components without losing stiffness capabilities. In the last years, it addresses other fields of applications with equally success. For that propose, several approaches have emerged in the last decades.

Initially, topology optimization has been successfully addressed through regularization techniques. The SIMP method represents probably the most celebrated strategy. The characteristic function, usually used to describe the weak (white) and stiff (black) subdomains, is regularized allowing intermediate values, or in other words, allowing the presence of gray areas. Frequently, this regularized representation of the characteristic is commonly named density function. Usually, the challenge is to characterize the material properties of the intermediate values of the density function (gray areas). This characterization is commonly described by an interpolation function. As referred in the work of Bendsøe and Sigmund,² the SIMP method proposes a polynomial interpolation function that, in some cases, lies inside the Hashin-Shtrikman (H-S) bounds. This could lead to gray areas that sometimes cannot be interpreted as microstructures. Additionally, depending on the nature of the materials, the SIMP method could propose a weak interpolation penalization, and consequently, large gray areas could appear.

This is an open access article under the terms of the Creative Commons Attribution License, which permits use, distribution, and reproduction in any medium, provided the original work is properly cited.

© 2019 The Authors. *International Journal for Numerical Methods in Engineering* Published by John Wiley & Sons, Ltd.

In this sense, novel projection methods have enabled promising black and white topologies.³ However, even not gray areas appear when using projection method, the final topology could be significantly suboptimal since it is influenced by the material properties provided by the corresponding interpolation. To circumvent this limitation and in order to fulfill the H-S bounds, other interpolation functions have been also proposed. Some examples can be found in the works of Stolpe and Svanberg⁴ and Dzierżanowski.⁵

Alternatively, due to the concept of shape derivative, shape optimization has also established as a reference strategy to solve topology optimization problems. Usually, the domain is described through a level-set function that, in turn, is advected using the shape derivative expression of the objective function. In this case, the shape derivative plays the role of the velocity field in the Hamilton-Jacobi equation.⁶ Although the algorithm requires considering initial holes, which can be increased and merged, resulting in new topologies during the iterations, the optimal shape presents no intermediate values and is clearly defined in the boundary.

Likewise, topological derivative addresses topology optimization with the intention of not considering intermediate values. The concept is based on studying the sensitivity of a functional when a circular (or ellipsoidal) inclusion of a weak material is inserted in a stiff material (or vice-versa). Through an asymptotic expansion and after solving an exterior problem, the obtained topological derivative closed formula certainly measures the adequacy or not of inserting in a certain point a weak/stiff inclusion. This valued concept is frequently exploited by level-set algorithms. The pioneer work of Amstutz and Andr a⁷ is a clear example. Other approaches can be found in the works of Allaire et al.⁸ and Yamada et al.⁹

Additionally, we can find in the literature the discrete and evolutionary algorithms, like BESO,¹⁰ as a competitive alternative to solve the problem. Although high efficiency is not clear for large problems, significant progress is achieved due to the increase of the available computational power. In the last years, other numerical techniques for decreasing the computational cost of topology optimization problems have been developed, like adaptive mesh refinement¹¹ and polytree-based adaptive polygonal finite element method.¹²

Although, at first sight, all the described approaches may seem very different, some connections have been observed in the work of Amstutz¹³ for the case of the topological derivative and the SIMP method approach, especially when the Poisson ratio of the stiff material is around 1/3. The present work follows and generalizes the results of that work. The first main result of the present work is to connect the topological derivative with the H-S bounds. This result allows us to have a new physical interpretation of the topological derivative concept. Then, based on the topological derivative, we propose the SIMP-ALL interpolation. Apart of being free of heuristic parameters, we show, as the second main result of this work, that it always remains in between the H-S bounds regardless the stiff and weak materials properties we want to interpolate. This result provides us a physical interpretation in terms of microstructures when using the SIMP-ALL interpolation. Note that proposing an interpolation strategy is convenient when the characteristic functions appears inside the differential operator. When this is not the case, no interpolation is needed, see for example, the work of S a et al.¹⁴

To validate the results, different cases are presented to compare SIMP-ALL with the SIMP interpolation functions and their relation with the H-S bounds. Finally, some numerical examples are computed to see the influence and convenience of the interpolation function on the optimal topologies. Additionally, a MATLAB code of the SIMP-ALL interpolation is provided.

This work is organized as follows. Section 2 presents the bimaterial topology optimization problem. Section 3 introduces the concept of the topological derivative and presents the topological derivative for isotropic materials in terms of the shear and bulk modulus. H-S bounds are briefly presented in Section 4 and connected with the topological derivative. The special kind of rational functions used in this work is defined in Section 5, and the SIMP-ALL interpolation function is presented in Section 6. Section 7 includes a comparison between SIMP and SIMP-ALL in relation with the H-S bounds. Additionally, some numerical examples are computed to observe the influence of the interpolation functions in the optimal topologies. The present work concludes in Section 8.

2 | TOPOLOGY OPTIMIZATION FORMULATION

2.1 | The exact topology optimization problem

Let Ω be a fixed domain split into Ω_1 and Ω_0 with enough regularity, fulfilling $\Omega_1 \cup \Omega_0 = \Omega$ and $\Omega_1 \cap \Omega_0 = \emptyset$. Let the boundary of Ω be defined as $\Gamma := \partial\Omega$ and split into Γ_D and Γ_N and let the spaces \mathcal{U} , \mathcal{V} , and \mathcal{X} be defined as

$$\mathcal{U} := \{\phi \in H^1(\Omega) : \phi|_{\Gamma_D} = u_0\}, \quad \mathcal{V} := \{\phi \in H^1(\Omega) : \phi|_{\Gamma_D} = 0\}, \quad \text{and} \quad \mathcal{X} := L^\infty(\Omega, \{0, 1\}). \quad (1)$$

Then, let us define the characteristic function $\chi \in \mathcal{X}$ and the fourth-order tensor $\mathbb{C}(\chi)$ as

$$\chi(x) = \begin{cases} 0 & x \in \Omega_0 \\ 1 & x \in \Omega_1 \end{cases} \quad \text{and} \quad \mathbb{C}(\chi) = (1 - \chi)\mathbb{C}_0 + \chi\mathbb{C}_1. \quad (2)$$

The constitutive tensors \mathbb{C}_0 and \mathbb{C}_1 in plane stress linear elasticity are defined as

$$\mathbb{C}_1 = 2\mu_1\mathbb{I} + (\kappa_1 - \mu_1)I \otimes I \quad \text{and} \quad \mathbb{C}_0 = 2\mu_0\mathbb{I} + (\kappa_0 - \mu_0)I \otimes I, \quad (3)$$

where \mathbb{I} and I represents the fourth- and second-order identity tensors and κ_1, μ_1 and κ_0, μ_0 are the bulk and shear modulus of the material in Ω_1 and in Ω_0 , respectively. Introducing the bilinear and linear form of the linear elasticity problem as

$$a(\chi, u, v) = \int_{\Omega} \nabla^s u : \mathbb{C}(\chi) : \nabla^s u \quad \text{and} \quad l(v) = \int_{\Gamma_N} t \cdot v, \quad (4)$$

the exact topology optimization problem can be then defined as follows: find $\chi \in \mathcal{X}$ and $u \in \mathcal{U}$ such that

$$\begin{aligned} \min_{\chi, u} \quad & J(\chi, u) = l(u) \\ \text{s.t.} \quad & \int_{\Omega} \chi \leq V \\ & a(\chi, u, v) = l(v) \quad \forall v \in \mathcal{V}, \end{aligned} \quad (5)$$

where, in this case, the cost $J(\chi, u)$ stands for the compliance function.

2.2 | The relaxed topology optimization problem

The difficulties of solving the exact problem are usually circumvented by proposing a relaxed version of it, this is by replacing the characteristic function with a density-like function $\rho(x) \in [0, 1]$, which, in contrast with the characteristic function, can take intermediate values. Thus, the exact topology optimization problem can be rewritten as the following regularized topology optimization problem: find $\rho \in \mathcal{R} = L^\infty(\Omega, [0, 1])$ and $u \in \mathcal{U}$ such that

$$\begin{aligned} \min_{\rho, u} \quad & J(\rho, u) = l(u) \\ \text{s.t.} \quad & \int_{\Omega} \rho \leq V \\ & a(\rho, u, v) = l(v) \quad \forall v \in \mathcal{V}, \end{aligned} \quad (6)$$

where the bilinear and linear form are now defined as

$$a(\rho, u, v) = \int_{\Omega} \nabla^s u : \mathbb{C}(\rho) : \nabla^s u \quad \text{and} \quad l(v) = \int_{\Gamma_N} t \cdot v. \quad (7)$$

In this case, the constitutive tensor takes the following form:

$$\mathbb{C}(\rho) = 2\mu(\rho)\mathbb{I} + (\kappa(\rho) - \mu(\rho))I \otimes I, \quad (8)$$

where $\mu(\rho) \in C^\infty([0, 1], [\mu_0, \mu_1])$ and $\kappa(\rho) \in C^\infty([0, 1], [\kappa_0, \kappa_1])$ are interpolation functions that must be proposed.

Computation of the compliance gradient. Let the compliance function $l(u)$ be defined as in (7) and let $u \in \mathcal{U}$ be the solution of the elasticity problem defined in (6), then the gradient of the compliance takes the following form:

$$g(\rho) = -\nabla^s u : \mathbb{C}'(\rho) : \nabla^s u, \quad (9)$$

where $\mathbb{C}'(\rho)$ is the derivative of the constitutive tensor defined in (8). To see this result, let us define the implicit function $F(\rho)$ as

$$F(\rho) = a(\rho, u(\rho), v) - l(v) = 0 \quad \forall v \in \mathcal{V}, \quad (10)$$

and let us compute its differential. From ellipticity arguments,¹⁵ we can state that $\forall v \in \mathcal{V}$ and $\forall \rho \in \mathcal{R}$ that provides a coercive constitutive tensor, there exists a unique $u \in \mathcal{U}$ that solves $a(\rho, u(\rho), v) = l(v)$. Thus, defining a density variation $\tilde{\rho} \in \mathcal{R}$, we can state that $F(\rho + \tilde{\rho}) - F(\rho) = 0$, and consequently,

$$\begin{aligned} F(\rho + \tilde{\rho}) - F(\rho) &= a(\rho + \tilde{\rho}, u(\rho + \tilde{\rho}), v) - a(\rho, u(\rho), v) \\ &= a(\rho + \tilde{\rho}, u(\rho + \tilde{\rho}), v) - a(\rho + \tilde{\rho}, u(\rho), v) + a(\rho + \tilde{\rho}, u(\rho), v) - a(\rho, u(\rho), v) \\ &= a(\rho + \tilde{\rho}, u(\rho)) + Du(\rho)\tilde{\rho}, v - a(\rho + \tilde{\rho}, u(\rho), v) + D_\rho a(\rho, u(\rho), v)\tilde{\rho} + o(\|\tilde{\rho}\|^2) \\ &= a(\rho + \tilde{\rho}, Du(\rho)\tilde{\rho}, v) + D_\rho a(\rho, u(\rho), v)\tilde{\rho} + o(\|\tilde{\rho}\|^2) \\ &= a(\rho, Du(\rho)\tilde{\rho}, v) + D_\rho a(\rho, u(\rho), v)\tilde{\rho} + o(\|\tilde{\rho}\|^2) = 0, \end{aligned} \quad (11)$$

where $D_\rho a(\rho, u(\rho), v)$ is the Fréchet derivative with respect to the first argument of the bilinear form $a(\rho, u, v)$ and $Du(\rho)$ is the Fréchet derivative of u at ρ . Then, the differential of the compliance can be computed as

$$\begin{aligned} l(u(\rho + \tilde{\rho})) - l(u(\rho)) &= a(\rho, u(\rho), D_\rho u(\rho)\tilde{\rho}) + o(\|\tilde{\rho}\|^2) = a(\rho, D_\rho u(\rho)\tilde{\rho}, u(\rho)) + o(\|\tilde{\rho}\|^2) \\ &= -D_\rho a(\rho, u(\rho), v)\tilde{\rho} + o(\|\tilde{\rho}\|^2) = -[a(\rho + \tilde{\rho}, u(\rho), v) - a(\rho, u(\rho), v)] + o(\|\tilde{\rho}\|^2) \\ &= -\int_{\Omega} \nabla^s u : (\mathbb{C}(\rho + \tilde{\rho}) - \mathbb{C}(\rho)) : \nabla^s u + o(\|\tilde{\rho}\|^2) \\ &= -\int_{\Omega} \nabla^s u : (\mathbb{C}'(\rho)\tilde{\rho}) : \nabla^s u + o(\|\tilde{\rho}\|^2) = Dl(\rho)\tilde{\rho} + o(\|\tilde{\rho}\|^2), \end{aligned} \quad (12)$$

where we have used the symmetric behavior of the bilinear form and the result of (11). Note that, for neglecting higher-order terms, we have supposed that the reminder $o(\|\tilde{\rho}\|^2)$ is small enough. The proof ends relating the gradient $g(\rho)$ of the compliance with its Fréchet derivative $Dl(u)$ by the Riesz representation theorem, ie, $Dl(\rho)\tilde{\rho} = \int_{\Omega} g\tilde{\rho}$.

3 | TOPOLOGICAL DERIVATIVE

On a given domain (unperturbed) $\Omega \subset \mathbb{R}^2$, let us insert in a certain point \hat{x} a small circular inclusion B_ε of radius $\varepsilon > 0$. We call the new (perturbed) domain Ω_ε (see in Figure 1).

Definition 1. Let $J(\Omega)$ and $J_\varepsilon(\Omega)$ be the value of a function in the unperturbed and perturbed domain. For a certain positive function $f(\varepsilon)$ such that $f(\varepsilon) \rightarrow 0$ when $\varepsilon \rightarrow 0$, typically, $f(\varepsilon) = \pi\varepsilon^2$, we define the topological derivative of $J(\Omega)$ as the following limit:

$$g_T(\hat{x}) = \lim_{\varepsilon \rightarrow 0^+} \frac{J_\varepsilon(\Omega) - J(\Omega)}{f(\varepsilon)}. \quad (13)$$

Remark 1. Note that to make expression (13) well defined, we need to ask that function $J_\varepsilon(\Omega)$ admits the following asymptotic expansion:

$$J_\varepsilon(\Omega) - J(\Omega) = f(\varepsilon)g_T(\hat{x}) + o(f(\varepsilon)). \quad (14)$$

Definition 2. For a given Young's modulus and Poisson's ratio of the matrix $\Omega_\varepsilon \setminus \overline{B_\varepsilon}$ and the inclusion B_ε , represented by E_m, ν_m and E_i, ν_i respectively, we define the fourth-order polarization tensor \mathbb{P} as

$$\mathbb{P} = p_1 \mathbb{I} + p_2 I \otimes I, \quad (15)$$

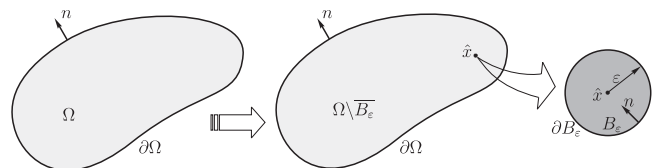


FIGURE 1 Topological derivative concept

where the parameters p_1 and p_2 take the following values:

$$p_1 = \frac{1}{\beta\gamma + \tau_1}(1 + \beta)(\tau_1 - \gamma) \quad \text{and} \quad p_2 = \frac{1}{2} \frac{(\alpha - \beta) [\gamma(\gamma - 2\tau_3) + \tau_1\tau_2]}{\beta\gamma + \tau_1} \frac{\alpha\gamma + \tau_2}{\alpha\gamma + \tau_2}, \quad (16)$$

and the coefficients $\alpha, \beta, \gamma, \tau_1, \tau_2$, and τ_3 are of the form

$$\alpha = \frac{1 + \nu_m}{1 - \nu_m}, \quad \beta = \frac{3 - \nu_m}{1 + \nu_m}, \quad \gamma = \frac{E_i}{E_m}, \quad (17)$$

$$\tau_1 = \frac{1 + \nu_i}{1 + \nu_m}, \quad \tau_2 = \frac{1 - \nu_i}{1 - \nu_m}, \quad \text{and} \quad \tau_3 = \frac{\nu_i(3\nu_m - 4) + 1}{\nu_m(3\nu_m - 4) + 1}. \quad (18)$$

Proposition 1. *Let $u \in \mathcal{U}$ be the solution of the elasticity problem defined in (6), let the compliance $l(u)$ be defined as in (7), and let the polarization tensor \mathbb{P} be expressed as in Definition 1, then the topological derivative at the point \hat{x} , defined as in Definition 1, is as follows:*

$$g_T(\hat{x}) = \sigma(\hat{x}) : \mathbb{P} : \nabla^s u(\hat{x}), \quad (19)$$

where ∇^s is the symmetric gradient operator and $\sigma = \mathbb{C}_m : \nabla^s u$ the stresses with \mathbb{C}_m the constitutive tensor of the matrix domain.

Proof. This result is not trivial and is obtained after proposing an asymptotic expansion of the solution of the topologically perturbed problem and after analytically solving an associated exterior problem. See the work of Novotny and Sokołowski¹⁶ for full details. For the same result but for any value of the Poisson ratio, see the work of Giusti et al.¹⁷ \square

For an easier comparison with the H-S bounds, we seek to rewrite the topological derivative only in terms of the shear and bulk modulus.

Topological derivative in terms of the shear and bulk modulus. Let us define the parameters $\eta_{\mu_m} = \frac{\kappa_m \mu_m}{2\mu_m + \kappa_m}$ and $\eta_{\kappa_m} = \mu_m$ in terms of the shear and bulk modulus of the matrix μ_m, κ_m and the insertion μ_i, κ_i and let us define the shear and bulk polarization parameters q_μ and q_κ as

$$q_\mu = q(\mu_m, \mu_i, \eta_{\mu_m}), \quad q_\kappa = q(\kappa_m, \kappa_i, \eta_{\kappa_m}) \quad \text{with} \quad q(t_1, t_2, t_3) = \frac{(t_1 + t_3)}{t_1(t_2 + t_3)}. \quad (20)$$

Then, the topological derivative in \hat{x} can be written only in terms of the shear and bulk modulus (of the matrix and inclusion) as follows:

$$g_T(\hat{x}) = -\nabla^s u(\hat{x}) : d\mathbb{C} : \nabla^s u(\hat{x}) \quad \text{with} \quad d\mathbb{C} = 2d\mu \mathbb{I} + [d\kappa - d\mu] I \otimes I, \quad (21)$$

where the parameters $d\mu$ and $d\kappa$ are

$$d\mu = \mu_m(\mu_i - \mu_m)q_\mu \quad \text{and} \quad d\kappa = \kappa_m(\kappa_i - \kappa_m)q_\kappa. \quad (22)$$

To obtain this expression, let the shear and bulk polarization coefficients q_μ and q_κ be computed first as

$$q_\mu = \frac{p_\mu}{(\mu_m - \mu_i)} \quad \text{and} \quad q_\kappa = \frac{p_\kappa}{(\kappa_m - \kappa_i)} \quad \text{with} \quad p_\mu = p_1 \quad \text{and} \quad p_\kappa = 2p_1 + p_2. \quad (23)$$

Inserting the lame parameters relations for plane stress $E = \frac{4\kappa\mu}{\kappa + \mu}$, and $\nu = \frac{\kappa - \mu}{\kappa + \mu}$ into the coefficients defined in (17) and (18) and replacing them in (16), we can write the shear and bulk polarization coefficients as follows:

$$q_\mu = \frac{\left(\mu_m + \frac{\kappa_m \mu_m}{2\mu_m + \kappa_m}\right)}{\mu_m \left(\mu_i + \frac{\kappa_m \mu_m}{2\mu_m + \kappa_m}\right)} \quad \text{and} \quad q_\kappa = \frac{(\kappa_m + \mu_m)}{\kappa_m(\kappa_i + \mu_m)}, \quad (24)$$

which are precisely $q(\mu_m, \mu_I, \eta_{\mu_m})$ and $q(\kappa_m, \kappa_I, \eta_{\kappa_m})$. Then, replacing relation (23) in (15), we can directly rewrite the polarization tensor as $\mathbb{P} = p_\mu \mathbb{I} + \frac{1}{2}(p_\kappa - p_\mu)I \otimes I$. The proof ends by replacing this last relation and the constitutive tensor of the matrix $\mathbb{C}_m = 2\mu_m \mathbb{I} + (\kappa_m - \mu_m)I \otimes I$ in the topological derivative expression (19).

Remark 2. We can clearly identify two different cases.

- (i) **Stiffer inclusion insertion:** We define this case by saying that, in a point $\hat{x} \in \Omega_0$ with parameters $\mu_m = \mu_0, \kappa_m = \kappa_0$, we add an inclusion with parameters $\mu_I = \mu_1$ and $\kappa_I = \kappa_1$. Then, the topological derivative g_{T_0} in this scenario takes in the point \hat{x} the following form:

$$g_{T_0}(\hat{x}) = -\nabla^s u(\hat{x}) : d\mathbb{C}_0 : \nabla^s u(\hat{x}), \quad (25)$$

with

$$d\mathbb{C}_0 = 2\mu_0(\mu_1 - \mu_0)q_{\mu_0} \mathbb{I} + [\kappa_0(\kappa_1 - \kappa_0)q_{\kappa_0} - \mu_0(\mu_1 - \mu_0)q_{\mu_0}] I \otimes I, \quad (26)$$

where $q_{\mu_0} = q(\mu_0, \mu_1, \eta_{\mu_0})$, $q_{\kappa_0} = q(\kappa_0, \kappa_1, \eta_{\kappa_0})$, $\eta_{\mu_0} = \frac{\kappa_0 \mu_0}{2\mu_0 + \kappa_0}$, and $\eta_{\kappa_0} = \mu_0$ are all positive values.

- (ii) **Weaker inclusion insertion:** Similarly, we define the opposite case by identifying in a point $\hat{x} \in \Omega_1$ the matrix parameters as $\mu_m = \mu_1, \kappa_m = \kappa_1$ and the parameters of the inclusion as $\mu_I = \mu_0$ and $\kappa_I = \kappa_0$. Then, the topological derivative g_{T_1} takes in the point \hat{x} the following form:

$$g_{T_1}(\hat{x}) = -\nabla^s u(\hat{x}) : d\mathbb{C}_1 : \nabla^s u(\hat{x}), \quad (27)$$

with

$$d\mathbb{C}_1 = 2\mu_1(\mu_0 - \mu_1)q_{\mu_1} \mathbb{I} + [\kappa_1(\kappa_0 - \kappa_1)q_{\kappa_1} - \mu_1(\mu_0 - \mu_1)q_{\mu_1}] I \otimes I, \quad (28)$$

where $q_{\mu_1} = q(\mu_1, \mu_0, \eta_{\mu_1})$, $q_{\kappa_1} = q(\kappa_1, \kappa_0, \eta_{\kappa_1})$, $\eta_{\mu_1} = \frac{\kappa_1 \mu_1}{2\mu_1 + \kappa_1}$ and $\eta_{\kappa_1} = \mu_1$ are also positive values.

Remark 3. Following the seminal work of Amstutz,¹³ one could think on proposing an interpolation scheme such that the gradient in Ω_1 and Ω_0 coincides precisely with the topological derivative. We distinguish again both scenarios.

- (i) **Stiffer inclusion insertion:** Take $\tilde{\rho} = \pi \varepsilon^2$ in $B(\hat{x}, \varepsilon)$ and zero otherwise, where $B(\hat{x}, \varepsilon)$ represents a small circular ball of center \hat{x} and radius ε . This means that, when replacing a small circular domain of the matrix by a small circular inclusion, we add a small amount of density. Then, if we want that Taylor's expansion (12) matches with the asymptotic expansion (14), we must define an interpolation such that, when $\tilde{x} \in \Omega_0$ ($\rho = 0$),

$$g(0) = g_{T_0}(\hat{x}) \quad \Rightarrow \quad \mathbb{C}'(0) = d\mathbb{C}_0 \quad \Rightarrow \quad \begin{cases} \mu'(0) = \mu_0(\mu_1 - \mu_0)q_{\mu_0} \\ \kappa'(0) = \kappa_0(\kappa_1 - \kappa_0)q_{\kappa_0}, \end{cases} \quad (29)$$

- (ii) **Weaker inclusion insertion:** In this case, we take $\tilde{\rho} = -\pi \varepsilon^2$ in $B(\hat{x}, \varepsilon)$ and zero otherwise. This means that, when replacing a small circular domain of the matrix by a small circular inclusion, we subtract a small amount of density. Similarly, to match both expansions, we should define an interpolation such that, when $\tilde{x} \in \Omega_1$ ($\rho = 1$),

$$-g(1) = g_{T_1}(\hat{x}) \quad \Rightarrow \quad \mathbb{C}'(1) = -d\mathbb{C}_1 \quad \Rightarrow \quad \begin{cases} \mu'(1) = \mu_1(\mu_1 - \mu_0)q_{\mu_1} \\ \kappa'(1) = \kappa_1(\kappa_1 - \kappa_0)q_{\kappa_1}. \end{cases} \quad (30)$$

4 | CONNECTION BETWEEN THE TOPOLOGICAL DERIVATIVE AND HASHIN-SHTRIKMAN BOUNDS

H-S bounds. Let us suppose that a composite material with shear and bulk constitutive properties μ^H and κ^H is composed by two-phase materials with a fraction volume $\rho \in [0, 1]$. Let us assume that the shear and bulk modulus of both constituents of the composite are μ_0 and κ_0 and μ_1 and κ_1 and satisfies $\kappa_1 > \kappa_0$. Then, the shear and bulk modulus of the

composite material μ^H and κ^H have an upper and lower bound regardless the arrangement of both phases. In addition, those bounds, commonly called isotropic H-S bounds, can be written, in the case of the shear modulus, as

$$\begin{aligned} \mu_{LB}(\rho) &= \mu_0(1 - \rho) + \mu_1\rho - \frac{(1 - \rho)\rho(\mu_1 - \mu_0)^2}{\mu_0\rho + \mu_1(1 - \rho) + \frac{\kappa_0\mu_0}{2\mu_0 + \kappa_0}} \\ \mu_{UB}(\rho) &= \mu_0(1 - \rho) + \mu_1\rho - \frac{(1 - \rho)\rho(\mu_1 - \mu_0)^2}{\mu_0\rho + \mu_1(1 - \rho) + \frac{\kappa_1\mu_1}{2\mu_1 + \kappa_1}} \end{aligned} \tag{31}$$

and similarly in the bulk modulus case as

$$\begin{aligned} \kappa_{LB}(\rho) &= \kappa_0(1 - \rho) + \kappa_1\rho - \frac{(1 - \rho)\rho(\kappa_1 - \kappa_0)^2}{\kappa_0\rho + \kappa_1(1 - \rho) + \mu_0} \\ \kappa_{UB}(\rho) &= \kappa_0(1 - \rho) + \kappa_1\rho - \frac{(1 - \rho)\rho(\kappa_1 - \kappa_0)^2}{\kappa_0\rho + \kappa_1(1 - \rho) + \mu_1} \end{aligned} \tag{32}$$

Those bounds were developed in the work of Hashin and Shtrikman.¹⁸ See also reference books by Bendsøe and Sigmund¹⁹ and Allaire.²⁰

Remark 4. Note that all bounds can be expressed in the following general form (generalized H-S bounds):

$$f_{HS}(\rho) = f_0(1 - \rho) + f_1\rho - \frac{(1 - \rho)\rho(f_1 - f_0)^2}{f_0\rho + f_1(1 - \rho) + \eta}, \tag{33}$$

where the shear and bulk H-S bounds are recovered by choosing the values described in the following table.

	μ_{LB}	μ_{UB}	κ_{LB}	κ_{UB}
f_0	μ_0	μ_0	κ_0	κ_0
f_1	μ_1	μ_1	κ_1	κ_1
η	$\eta_{\mu_0} = \frac{\kappa_0\mu_0}{2\mu_0 + \kappa_0}$	$\eta_{\mu_1} = \frac{\kappa_1\mu_1}{2\mu_1 + \kappa_1}$	$\eta_{\kappa_0} = \mu_0$	$\eta_{\kappa_1} = \mu_1$

(34)

Remark 5. Note that the derivative of the H-S bounds in both components can be rewritten as follows:

$$\left\{ \begin{aligned} \mu'_{LB}(0) &= \mu_0(\mu_1 - \mu_0)q_{\mu_0} \\ \mu'_{UB}(1) &= \mu_1(\mu_1 - \mu_0)q_{\mu_1} \end{aligned} \right. \quad \text{and} \quad \left\{ \begin{aligned} \kappa'_{LB}(0) &= \kappa_0(\kappa_1 - \kappa_0)q_{\kappa_0} \\ \kappa'_{UB}(1) &= \kappa_1(\kappa_1 - \kappa_0)q_{\kappa_1} \end{aligned} \right. \tag{35}$$

In fact, this way of rewriting the H-S bounds derivative can be obtained after simple calculations. From Equation (33), the generalized H-S bound can be rewritten as

$$f_{HS}(\rho) = \frac{f_0 d_0^{HS}(1 - \rho) + f_1 d_1^{HS} \rho}{d_0^{HS}(1 - \rho) + d_1^{HS} \rho} \quad \text{with} \quad d_0^{HS} = \frac{(f_1 - f_0)^2}{f_0 + \eta}, \quad d_1^{HS} = \frac{(f_1 - f_0)^2}{f_1 + \eta}, \tag{36}$$

and consequently, the derivative of the generalized H-S bounds is expressed as

$$f'_{HS}(\rho) = \frac{d_0^{HS} d_1^{HS} (f_1 - f_0)}{[d_0^{HS}(1 - \rho) + d_1^{HS} \rho]^2}. \tag{37}$$

Thus, its value in the components is just

$$\begin{aligned} f'_{HS}(0) &= \frac{d_1^{HS}}{d_0^{HS}}(f_1 - f_0) = \frac{f_0 + \eta}{f_1 + \eta}(f_1 - f_0) \\ f'_{HS}(1) &= \frac{d_0^{HS}}{d_1^{HS}}(f_1 - f_0) = \frac{f_1 + \eta}{f_0 + \eta}(f_1 - f_0). \end{aligned} \quad (38)$$

Inserting (34) into (37) and using definition of q in (20), the derivative of the H-S bounds for the shear modulus in Ω_0 ($\rho = 0$) and in Ω_1 ($\rho = 1$) are

$$\begin{aligned} \mu'_{LB}(0) &= \frac{(\mu_0 + \eta_{\mu_0})(\mu_1 - \mu_0)}{\mu_1 + \eta_{\mu_0}} = -\mu_0(\mu_0 - \mu_1)q(\mu_0, \mu_1, \eta_{\mu_0}) = \mu_0(\mu_1 - \mu_0)q_{\mu_0} \\ \mu'_{LB}(1) &= \frac{(\mu_1 + \eta_{\mu_0})(\mu_1 - \mu_0)}{\mu_0 + \eta_{\mu_0}} = \mu_1(\mu_1 - \mu_0)q(\mu_1, \mu_0, \eta_{\mu_0}) \\ \mu'_{UB}(0) &= \frac{(\mu_0 + \eta_{\mu_1})(\mu_1 - \mu_0)}{\mu_1 + \eta_{\mu_1}} = -\mu_0(\mu_0 - \mu_1)q(\mu_0, \mu_1, \eta_{\mu_1}) \\ \mu'_{UB}(1) &= \frac{(\mu_1 + \eta_{\mu_1})(\mu_1 - \mu_0)}{\mu_0 + \eta_{\mu_1}} = \mu_1(\mu_1 - \mu_0)q(\mu_1, \mu_0, \eta_{\mu_1}) = \mu_1(\mu_1 - \mu_0)q_{\mu_1}. \end{aligned} \quad (39)$$

Similarly, the derivative of the H-S bounds for the bulk modulus in Ω_0 ($\rho = 0$) and in Ω_1 ($\rho = 1$) can be written as

$$\begin{aligned} \kappa'_{LB}(0) &= \frac{(\kappa_0 + \eta_{\kappa_0})(\kappa_1 - \kappa_0)}{\kappa_1 + \eta_{\kappa_0}} = -\kappa_0(\kappa_0 - \kappa_1)q(\kappa_0, \kappa_1, \eta_{\kappa_0}) = \kappa_0(\kappa_1 - \kappa_0)q_{\kappa_0} \\ \kappa'_{LB}(1) &= \frac{(\kappa_1 + \eta_{\kappa_0})(\kappa_1 - \kappa_0)}{\kappa_0 + \eta_{\kappa_0}} = \kappa_1(\kappa_1 - \kappa_0)q(\kappa_1, \kappa_0, \eta_{\kappa_0}) \\ \kappa'_{UB}(0) &= \frac{(\kappa_0 + \eta_{\kappa_1})(\kappa_1 - \kappa_0)}{\kappa_1 + \eta_{\kappa_1}} = -\kappa_0(\kappa_0 - \kappa_1)q(\kappa_0, \kappa_1, \eta_{\kappa_1}) \\ \kappa'_{UB}(1) &= \frac{(\kappa_1 + \eta_{\kappa_1})(\kappa_1 - \kappa_0)}{\kappa_0 + \eta_{\kappa_1}} = \kappa_1(\kappa_1 - \kappa_0)q(\kappa_1, \kappa_0, \eta_{\kappa_1}) = \kappa_1(\kappa_1 - \kappa_0)q_{\kappa_1}. \end{aligned} \quad (40)$$

Topological derivative as H-S bounds derivative. This is one of the two main results of this work. Let us define two material components with shear and bulk material properties μ_0, κ_0 and μ_1, κ_1 , respectively, and let us propose an interpolation function for modeling its mixture by means of its fraction volume $\rho = [0, 1]$ such that close to Ω_0 coincides with the H-S lower bound and close to Ω_1 with the H-S upper bound. Then, the gradient of the compliance coincides with the topological derivative in Ω_0 and Ω_1 .

To see this result, from Equation (9), we can write the gradient of the compliance (when using the isotropic lower and upper bound as interpolation function) as follows:

$$\begin{aligned} g_{LB}(0) &= -\nabla^s u : \mathbb{C}'_{LB}(0) : \nabla^s u \quad \text{with} \quad \mathbb{C}_{LB}(\rho) = 2\mu_{LB}(\rho)\mathbb{I} + [\kappa_{LB}(\rho) - \mu_{LB}(\rho)]I \otimes I \\ g_{UB}(1) &= -\nabla^s u : \mathbb{C}'_{UB}(1) : \nabla^s u \quad \text{with} \quad \mathbb{C}_{UB}(\rho) = 2\mu_{UB}(\rho)\mathbb{I} + [\kappa_{UB}(\rho) - \mu_{UB}(\rho)]I \otimes I. \end{aligned} \quad (41)$$

Then, we can identify coefficients in (39) and (40) with precisely the ones established by the topological derivative in (29) and (30), and thus,

$$\begin{cases} \mathbb{C}'_{LB}(0) = d\mathbb{C}_0 & \text{when } \tilde{x} \in \Omega_0 \\ \mathbb{C}'_{UB}(1) = d\mathbb{C}_1 & \text{when } \tilde{x} \in \Omega_1. \end{cases} \quad (42)$$

Finally, using (42) in Equations (25), (27), and (9), we obtain

$$\begin{cases} g_{LB}(0) = g_{T_0}(\tilde{x}) & \text{when } \tilde{x} \in \Omega_0 \\ g_{UB}(1) = g_{T_1}(\tilde{x}) & \text{when } \tilde{x} \in \Omega_1. \end{cases} \quad (43)$$

Remark 6. This result confirms that the material in the neighborhood of the infinitesimal inclusion inserted in the perturbed domain used to compute the topological derivative can be understood as an homogenized microstructure with circular inclusions (H-S bounds microstructures) with a fraction volume value equivalent to the infinitesimal inclusion volume. This is to say that, in order to study a change on the compliance, the topological derivative concepts proposes in fact to insert H-S microstructures.

5 | RATIONAL FUNCTIONS

Definition 3. Let us introduce the following particular family of rational functions:

$$\mathcal{R} = \left\{ f \in C^\infty([0, 1], [f_0, f_1]) \mid f(\rho) = \frac{A\rho^2 + B\rho + C}{D\rho + 1} \right\}, \quad (44)$$

where A, B, C , and $D \neq -1$ are scalar parameters to be determined by fixing the value and its derivative in the extremes, ie,

$$f(0) = f_0, \quad f'(0) = \dot{f}_0, \quad f(1) = f_1, \quad \text{and} \quad f'(1) = \dot{f}_1. \quad (45)$$

Remark 7. Note that function $f \in \mathcal{R}$ is equivalent to the following expression:

$$f(\rho) = \frac{d_{01}(1 - \rho)\rho + f_0d_0(1 - \rho) + f_1d_1\rho}{d_0(1 - \rho) + d_1\rho} \quad \text{with} \quad \begin{cases} d_{01} = \dot{f}_1\dot{f}_0 - (f_1 - f_0)^2 \\ d_0 = \dot{f}_1 - (f_1 - f_0) \\ d_1 = (f_1 - f_0) - \dot{f}_0. \end{cases} \quad (46)$$

This result is easily obtained by computing the derivative of the rational function as

$$f'(\rho) = \frac{AD\rho^2 + 2A\rho + (B - CD)}{(D\rho + 1)^2} \quad (47)$$

and imposing conditions (45). Then, we can solve the system of four equations to find the value of the parameters A, B, C , and D . This is

$$A = \frac{-\dot{f}_1\dot{f}_0 + (f_1 - f_0)^2}{\dot{f}_1 + (f_1 - f_0)}, \quad B = \frac{2f_0(f_1 - f_0) + \dot{f}_1\dot{f}_0 - f_1\dot{f}_0 - \dot{f}_1f_0}{\dot{f}_1 + (f_1 - f_0)}, \quad C = f_0, \quad \text{and} \quad D = \frac{2(f_1 - f_0) - (\dot{f}_1 + \dot{f}_0)}{\dot{f}_1 + (f_1 - f_0)}. \quad (48)$$

Remark 8. Note that, with the definitions above, the following property holds: $d_{01} = (f_1 - f_0)(d_0 - d_1) - d_0d_1$.

Remark 9. The generalized H-S bounds and therefore the upper and lower bounds of the shear and bulk modulus are rational functions. This can be easily seen by imposing

$$d_{01} = 0, \quad d_0 = d_0^{HS} = \frac{(f_1 - f_0)^2}{f_0 + \eta}, \quad \text{and} \quad d_1 = d_1^{HS} = \frac{(f_1 - f_0)^2}{f_1 + \eta} \quad (49)$$

in the general rational Equation (46) and obtaining

$$f_{HS}(\rho) = \frac{f_0d_0^{HS}(1 - \rho) + f_1d_1^{HS}\rho}{d_0^{HS}(1 - \rho) + d_1^{HS}\rho}, \quad (50)$$

which is precisely the generalized H-S equation (33).

6 | SIMP-ALL METHOD

The idea of the SIMP-ALL method is precisely to propose an interpolation such that the gradient of the compliance coincides with the topological derivative in both Ω_0 and Ω_1 . As already shown in Equation (43), in the case of isotropic materials, this is equivalent to impose the derivative of the H-S lower bound in Ω_0 and the derivative of the H-S upper bound in Ω_1 for the shear and bulk modulus interpolations.

Definition 4. The SIMP-ALL function $f_{SA}(\rho)$ is defined as a rational function \mathcal{R} with the H-S bound derivatives (lower in $\rho = 0$ and upper in $\rho = 1$) as derivative parameters \dot{f}_0 and \dot{f}_1 . This is

$$\dot{f}_0 = f'_{HS}(0) = \frac{f_0 + \eta_0}{f_1 + \eta_0}(f_1 - f_0) \quad \text{and} \quad \dot{f}_1 = f'_{HS}(1) = \frac{f_1 + \eta_1}{f_0 + \eta_1}(f_1 - f_0). \quad (51)$$

Remark 10. Note that the shear and bulk SIMP-ALL interpolation function $\mu_{SA}(\rho)$ and $\kappa_{SA}(\rho)$ can be rewritten in the following compact form:

$$\begin{aligned} \mu_{SA}(\rho) &= \frac{(\mu_1 - \mu_0)(\eta_{\mu_0} - \eta_{\mu_1})(1 - \rho)\rho + \mu_0(\mu_1 + \eta_{\mu_0})(1 - \rho) + \mu_1(\mu_0 + \eta_{\mu_1})\rho}{(\mu_1 + \eta_{\mu_0})(1 - \rho) + (\mu_0 + \eta_{\mu_1})\rho} \\ \kappa_{SA}(\rho) &= \frac{(\kappa_1 - \kappa_0)(\eta_{\kappa_0} - \eta_{\kappa_1})(1 - \rho)\rho + \kappa_0(\kappa_1 + \eta_{\kappa_0})(1 - \rho) + \kappa_1(\kappa_0 + \eta_{\kappa_1})\rho}{(\kappa_1 + \eta_{\kappa_0})(1 - \rho) + (\kappa_0 + \eta_{\kappa_1})\rho}, \end{aligned} \quad (52)$$

where $\eta_{\mu_0} = \frac{\kappa_0\mu_0}{2\mu_0 + \kappa_0}$, $\eta_{\mu_1} = \frac{\kappa_1\mu_1}{2\mu_1 + \kappa_1}$, $\eta_{\kappa_0} = \mu_0$, and $\eta_{\kappa_1} = \mu_1$ were previously defined in (34).

These expressions can be easily obtained by computing the rational function parameters d_{01} , d_0 , and d_1 defined in Equation (46). In the case of the SIMP-ALL interpolation, they can be written as

$$\begin{aligned} d_{01}^{SA} &= \dot{f}_1 \dot{f}_0 - (f_1 - f_0)^2 = (f_1 - f_0)^2 \left(\frac{f_0 + \eta_0}{f_1 + \eta_0} \frac{f_1 + \eta_1}{f_0 + \eta_1} - 1 \right) \\ &= \frac{(f_1 - f_0)^3 (\eta_0 - \eta_1)}{(f_0 + \eta_1)(f_1 + \eta_0)} \\ d_0^{SA} &= \dot{f}_1 - (f_1 - f_0) = (f_1 - f_0) \left(\frac{f_1 + \eta_1}{f_0 + \eta_1} - 1 \right) = \frac{(f_1 - f_0)^2}{f_0 + \eta_1} \\ d_1^{SA} &= (f_1 - f_0) - \dot{f}_0 = (f_1 - f_0) \left(1 - \frac{f_0 + \eta_0}{f_1 + \eta_0} \right) = \frac{(f_1 - f_0)^2}{f_1 + \eta_0}. \end{aligned} \quad (53)$$

These parameters let us build the SIMP-ALL general interpolation function $f^{SA}(\rho)$ as

$$\begin{aligned} f_{SA}(\rho) &= \frac{d_{01}^{SA}(1 - \rho)\rho + f_0 d_0^{SA}(1 - \rho) + f_1 d_1^{SA}\rho}{d_0^{SA}(1 - \rho) + d_1^{SA}\rho} \\ &= \frac{(f_1 - f_0)(\eta_0 - \eta_1)(1 - \rho)\rho + f_0(f_1 + \eta_0)(1 - \rho) + f_1(f_0 + \eta_1)\rho}{(f_1 + \eta_0)(1 - \rho) + (f_0 + \eta_1)\rho}, \end{aligned} \quad (54)$$

where the last expression is obtained multiplying the upper and lower parts of the fraction by $\frac{(f_0 + \eta_1)(f_1 + \eta_0)}{(f_1 - f_0)^2}$. Finally, we have to take the corresponding f_0, f_1, η_0 , and η_1 parameters values for the case of the shear and bulk modulus.

Difference of two rational functions. Let $f_A \in \mathcal{R}$ and $f_B \in \mathcal{R}$ be two rational functions such that $f'_B(0) \leq f'_A(0)$, $f'_A(1) \leq f'_B(1)$, $f_A(0) = f_B(0)$, and $f_A(1) = f_B(1)$ for all $\rho \in [0, 1]$. Then,

$$f_A(\rho) \geq f_B(\rho) \quad \forall \rho \in [0, 1]. \quad (55)$$

To obtain this result, we will show in four steps that the difference of f_A and f_B is positive $\forall \rho \in [0, 1]$.

(i) **Computing the difference function.** Let us compute the function f_C as the difference of the two rational functions f_A and f_B . This is

$$f_C(\rho) = f_A(\rho) - f_B(\rho) = \frac{n_C(\rho)}{d_C(\rho)}, \tag{56}$$

where the numerator $n_C(\rho)$ is written as

$$n_C(\rho) = n_A(\rho)d_B(\rho) - n_B(\rho)d_A(\rho) \quad \text{with} \quad \begin{cases} n_A(\rho) = d_{01}^A(1 - \rho)\rho + f_0d_0^A(1 - \rho) + f_1d_1^A\rho \\ n_B(\rho) = d_{01}^B(1 - \rho)\rho + f_0d_0^B(1 - \rho) + f_1d_1^B\rho \end{cases} \tag{57}$$

and the denominator $d_C(\rho)$ as

$$d_C(\rho) = d_A(\rho)d_B(\rho) \quad \text{with} \quad \begin{cases} d_A(\rho) = d_0^A(1 - \rho) + d_1^A\rho \\ d_B(\rho) = d_0^B(1 - \rho) + d_1^B\rho. \end{cases} \tag{58}$$

(ii) **Computing the difference function numerator.** For sake of compactness, we write the numerator in matrix form as

$$\begin{aligned} n_C(\rho) &= \begin{bmatrix} (1 - \rho)\rho & (1 - \rho) & \rho \end{bmatrix} \left(\begin{bmatrix} d_{01}^A \\ f_0d_0^A \\ f_1d_1^A \end{bmatrix} \begin{bmatrix} d_0^B & d_1^B \end{bmatrix} - \begin{bmatrix} d_{01}^B \\ f_0d_0^B \\ f_1d_1^B \end{bmatrix} \begin{bmatrix} d_0^A & d_1^A \end{bmatrix} \right) \begin{bmatrix} (1 - \rho) \\ \rho \end{bmatrix} = \\ &= \begin{bmatrix} (1 - \rho)\rho & (1 - \rho) & \rho \end{bmatrix} \begin{bmatrix} d_{01}^A d_0^B - d_{01}^B d_0^A & d_{01}^A d_1^B - d_{01}^B d_1^A \\ f_0 d_0^A d_0^B - f_0 d_0^B d_0^A & f_0 d_0^A d_1^B - f_0 d_0^B d_1^A \\ f_1 d_1^A d_0^B - f_1 d_1^B d_0^A & f_1 d_1^A d_1^B - f_1 d_1^B d_1^A \end{bmatrix} \begin{bmatrix} (1 - \rho) \\ \rho \end{bmatrix} = \\ &= \begin{bmatrix} (1 - \rho)\rho & (1 - \rho) & \rho \end{bmatrix} \begin{bmatrix} N_{11} & N_{12} \\ 0 & N_{22} \\ N_{31} & 0 \end{bmatrix} \begin{bmatrix} (1 - \rho) \\ \rho \end{bmatrix} = \\ &= (1 - \rho)^2 \rho N_{11} + (1 - \rho) \rho^2 N_{12} + (1 - \rho) \rho N_{22} + \rho (1 - \rho) N_{31} = \\ &= (1 - \rho) \rho \left[(1 - \rho) N_{11} + \rho N_{12} + N_{22} + N_{31} \right] \\ &= (1 - \rho) \rho \left[(1 - \rho) (N_{11} + N_{22} + N_{31}) + \rho (N_{12} + N_{22} + N_{31}) \right] \\ &= (1 - \rho) \rho \left[(1 - \rho) c_0 + \rho c_1 \right], \end{aligned} \tag{59}$$

where $c_0 = N_{11} + N_{22} + N_{31}$ and $c_1 = N_{12} + N_{22} + N_{31}$. Note that, from Remark 8, N_{11} , N_{12} , N_{22} , and N_{31} can be written as

$$\begin{aligned} N_{11} &= [(f_1 - f_0)(d_0^A - d_1^A) - d_0^A d_1^A] d_0^B - [(f_1 - f_0)(d_0^B - d_1^B) - d_0^B d_1^B] d_0^A = \\ &= -(f_1 - f_0)(d_0^B d_1^A - d_1^B d_0^A) + (d_1^B - d_1^A) d_0^A d_0^B \\ N_{12} &= [(f_1 - f_0)(d_0^A - d_1^A) - d_0^A d_1^A] d_1^B - [(f_1 - f_0)(d_0^B - d_1^B) - d_0^B d_1^B] d_1^A = \\ &= -(f_1 - f_0)(d_0^B d_1^A - d_1^B d_0^A) + (d_0^B - d_0^A) d_1^A d_1^B \\ N_{22} &= -f_0 (d_0^B d_1^A - d_1^B d_0^A) \\ N_{31} &= -f_1 (d_0^B d_1^A - d_1^B d_0^A). \end{aligned} \tag{60}$$

and the sum of N_{22} and N_{31} as $N_{22} + N_{31} = (f_1 - f_0)(d_0^B d_1^A - d_1^B d_0^A)$. Thus, we can write coefficients c_0 and c_1 in a simplified form as

$$\begin{aligned} c_0 &= (d_1^B - d_1^A) d_0^A d_0^B, \\ c_1 &= (d_0^B - d_0^A) d_1^A d_1^B. \end{aligned} \tag{61}$$

(iii) **Computing the difference function denominator.** From Equation (58), this is simply

$$d_C(\rho) = [d_0^A(1 - \rho) + d_1^A\rho] [d_0^B(1 - \rho) + d_1^B\rho]. \quad (62)$$

(iv) **Positiveness of the difference for all possible scenarios.** The idea is now to analyze if the numerator and the denominator of the difference have always the same sign in all possible cases. First, note that, since $f_A \in \mathcal{R}$ and $f_B \in \mathcal{R}$, their image should not be unbounded (should be between $[f_0, f_1]$). Thus, from (62), we see that the following two scenarios are only possible:

$$d_0, d_1 > 0 \quad \text{or} \quad d_0, d_1 < 0. \quad (63)$$

Then, the assumptions of $f'_B(0) \leq f'_A(0)$ and $f'_A(1) \leq f'_B(1)$ entail the following inequalities:

$$\begin{aligned} f'_B(0) - f'_A(0) &= [(f_1 - f_0) - d_1^B] - [(f_1 - f_0) - d_1^A] = d_1^A - d_1^B \leq 0 &\implies d_1^B \geq d_1^A \\ f'_A(1) - f'_B(1) &= [(f_1 - f_0) + d_0^A] - [(f_1 - f_0) + d_0^B] = d_0^A - d_0^B \leq 0 &\implies d_0^B \geq d_0^A. \end{aligned} \quad (64)$$

In view of (64), we summarize all the possible scenarios in the following table.

	$d_0^B \geq d_0^A \geq 0$	$d_0^B \geq 0 \geq d_0^A$	$0 \geq d_0^B \geq d_0^A$
$d_1^B \geq d_1^A \geq 0$	Case 1	Not possible	Not possible
$d_1^B \geq 0 \geq d_1^A$	Not possible	Case 2	Not possible
$0 \geq d_1^B \geq d_1^A$	Not possible	Note possible	Case 3

(65)

In the table, Cases 1, 2, and 3 are the only possible cases that makes f_A and f_B satisfy condition (63), and consequently, the rest of cases are not included. Thus, we can guarantee positiveness of function f_C reasoning as follows:

$$\begin{aligned} \text{Case 1: } &\begin{cases} c_1, c_0 > 0 \\ d_A(\rho) > 0, d_B(\rho) > 0 \end{cases} &\implies n_C(\rho) > 0 &\implies d_C(\rho) > 0 &\implies f_C(\rho) > 0 \quad \forall \rho \in [0, 1] \\ \text{Case 2: } &\begin{cases} c_1, c_0 < 0 \\ d_A(\rho) < 0, d_B(\rho) > 0 \end{cases} &\implies n_C(\rho) < 0 &\implies d_C(\rho) < 0 &\implies f_C(\rho) > 0 \quad \forall \rho \in [0, 1] \\ \text{Case 3: } &\begin{cases} c_1, c_0 > 0 \\ d_A(\rho) > 0, d_B(\rho) < 0 \end{cases} &\implies n_C(\rho) > 0 &\implies d_C(\rho) > 0 &\implies f_C(\rho) > 0 \quad \forall \rho \in [0, 1]. \end{aligned} \quad (66)$$

Remark 11. Based on the results shown above, although it may be obvious, we could show that the H-S upper bound is above the H-S lower bound. Indeed,

$$f'_{UB}(0) - f'_{LB}(0) = \frac{f_0 + \eta_1}{f_1 + \eta_1}(f_1 - f_0) - \frac{f_0 + \eta_0}{f_1 + \eta_0}(f_1 - f_0) = \frac{(f_1 - f_0)^2(\eta_1 - \eta_0)}{(f_1 + \eta_0)(f_1 + \eta_0)} \geq 0 \quad (67)$$

$$f'_{LB}(1) - f'_{UB}(1) = \frac{f_1 + \eta_0}{f_0 + \eta_0}(f_1 - f_0) - \frac{f_1 + \eta_1}{f_0 + \eta_1}(f_1 - f_0) = \frac{(f_1 - f_0)^2(\eta_1 - \eta_0)}{(f_0 + \eta_0)(f_0 + \eta_1)} \geq 0, \quad (68)$$

where we have used $f_1, f_0 \geq 0$ for coercivity reasons and $\eta_1 \geq 0, \eta_0 \geq 0$ is fulfilled by definition from table (34) for both the shear and the bulk modulus. Thus, as expected, the H-S bound for both the shear and bulk modulus is always above the H-S lower bound. This is

$$\mu_{UB}(\rho) \geq \mu_{LB}(\rho) \quad \text{and} \quad \kappa_{UB}(\rho) \geq \kappa_{LB}(\rho) \quad \forall \rho \in [0, 1]. \quad (69)$$

SIMP-ALL in between H-S bounds. At this point, we can show that the SIMP-ALL interpolation for the bulk and shear modulus rest always between the H-S bounds, this is

$$\mu_{UB}(\rho) \geq \mu_{SA}(\rho) \geq \mu_{LB}(\rho) \quad \text{and} \quad \kappa_{UB}(\rho) \geq \kappa_{SA}(\rho) \geq \kappa_{LB}(\rho) \quad \forall \rho \in [0, 1]. \quad (70)$$

This result is certainly the second main contribution of this work. To show it, we only have to verify the conditions stated before Equation (55). In fact, the H-S upper bound and the SIMP-ALL interpolation function fulfills by construction

$$f'_{UB}(0) - f'_{SA}(0) = f'_{UB}(0) - f'_{LB}(0) \geq 0 \quad \text{and} \quad f'_{SA}(1) - f'_{UB}(1) = 0. \quad (71)$$

Condition $f'_{UB}(0) - f'_{LB}(0) \geq 0$ has been already shown in (67). We can proceed similarly for the H-S lower bound. By construction,

$$f'_{SA}(0) - f'_{LB}(0) = 0 \quad \text{and} \quad f'_{SA}(1) - f'_{UB}(1) = f'_{LB}(1) - f'_{UB}(1) \geq 0, \quad (72)$$

and condition $f'_{SA}(1) - f'_{UB}(1) = f'_{LB}(1) - f'_{UB}(1) \geq 0$ has been also already proven in (67).

7 | COMPARISON BETWEEN SIMP AND SIMP-ALL

The celebrated SIMP interpolation function¹⁹ proposes basically to combine the property of both materials as follows:

$$\mathbb{C}(\rho) = (1 - \rho^p)\mathbb{C}_0 + \rho^p\mathbb{C}_1, \quad (73)$$

where p is the penalization parameter, frequently taken as $p = 3$.

7.1 | Interpolation function comparison

We seek in this section to compare both interpolations in the following two different situations.

(a) Material-void interpolation

In regularized topology optimization, the material of the domain (base material) is usually interpolated with a *void* material, modeled with an extremely weak material. As discussed in the work of Bendsøe and Sigmund,² standard SIMP proposes an isotropic interpolation, which its corresponding intermediate values (gray) cannot be interpreted in some situations as a composite material composed by the base material and the *void* material (the interpolation function remains outside the H-S bounds). To circumvent this limitation, an adaptive value of the penalization parameter (in terms of the Poisson ratio value of the base material ν_1) is proposed in the aforementioned work² for two-dimensional plane stress cases by changing the penalization parameter as follows:

$$p \geq p^*(\nu_1) = \max\left(\frac{2}{1 - \nu_1}, \frac{4}{1 + \nu_1}\right). \quad (74)$$

With this adaptation of the penalization parameter, the SIMP method remains in between the H-S bounds when $\mu_0 \rightarrow 0$ and $\kappa_0 \rightarrow 0$. In the following, we will call this interpolation choice as adaptive SIMP. For comparing SIMP, SIMP-ALL, and adaptive SIMP, in this work, we have proposed a sequence of composite materials composed by an isotropic base material with properties ($E_1 = 1$, $\nu_1 \in \{1/3, 0, -0.5, -0.75, -0.9\}$) and a void material with properties ($E_0 = 10^{-3}$, $\nu_0 = 1/3$). Note that the value of ν_0 when $E_0 \rightarrow 0$ has no relevance.

The SIMP, adaptive SIMP, and SIMP-ALL interpolation function have been depicted in Figure 2 in relation with the shear and bulk H-S bounds. In view of the results, when the Poisson ratio is $\nu = 1/3$, the three interpolations behave similarly. In fact, SIMP adaptive and SIMP coincides since $p^*(1/3) = 3$. Additionally, both the SIMP and the

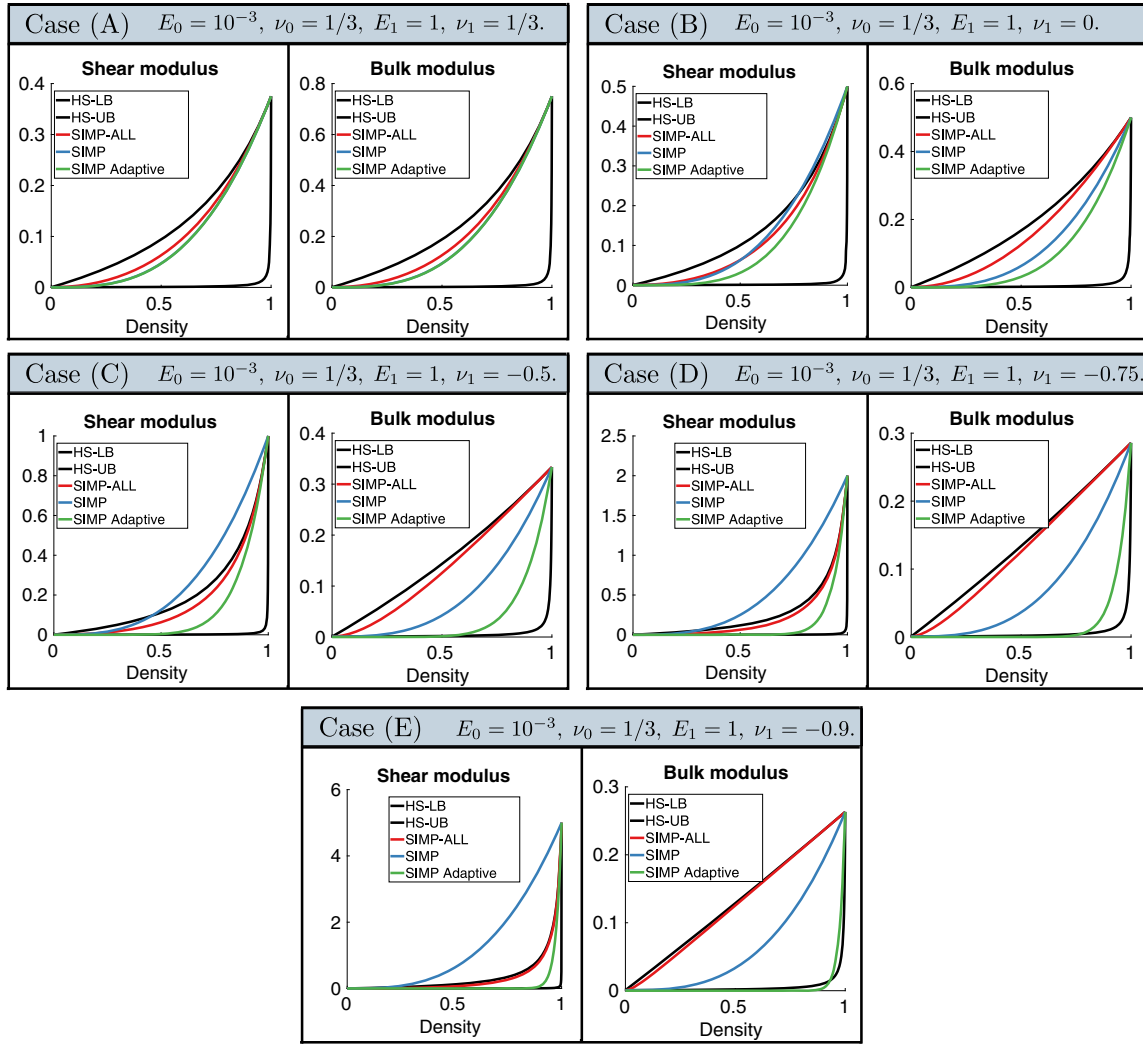


FIGURE 2 Shear and bulk interpolation function comparison when interpolating *void* material ($E_0 = 10^{-3}$, $\nu_0 = 1/3$) with a sequence of *stiff* materials ($E_1 = 1$ and ν_1 decreasing). In contrast with SIMP, SIMP adaptive, and SIMP-ALL interpolations remain in between H-S bounds

SIMP-ALL interpolation function take the H-S bounds derivative values in the extreme values (the lower bound in $\rho = 0$ and the upper bound in $\rho = 1$). The former coincidence is proved in the work of Bendsoe and Sigmund¹⁹ while the latter is obtained by construction. In this case, both interpolation remain in between the H-S bounds. However, as soon as ν_1 decreases, SIMP, SIMP adaptive, and SIMP-ALL start differing. In fact, SIMP-ALL and SIMP adaptive interpolation function, in contrast with SIMP, remain in between H-S bounds as expected. Additionally, note that as soon as ν_1 decreases, eg, $\nu_1 = -0.9$, $p^* = 40$ (Case (E)), the adaptive SIMP interpolation, in comparison with the SIMP-ALL interpolation, increases extremely markedly resulting in possible limitations when solving topology optimization problems.

(b) Bimaterial interpolation

For a more general case, when the weak material is not necessary much less stiff than the base material, the topology optimization problem is in fact a bimaterial optimization problem. The aim is to decide in which part of Ω is appropriate to use one material or the other, or in case of “grays,” a combination of both. Two different cases have been presented. The first one (Case (A)) seeks to model an Steel-Aluminum composite. In this sense, the material properties have been taken as $E_0 = 1/3$, $\nu_0 = 0.35$, $E_1 = 1$, and $\nu_1 = 0.3$. The second example (Case (B)) intends to model an extreme case where one material has larger bulk modulus value and the other material has larger shear modulus value. To this aim, the material properties considered are $E_0 = 0.9$, $\nu_0 = -0.9$, $E_1 = 1$, and $\nu_1 = 0.3$.

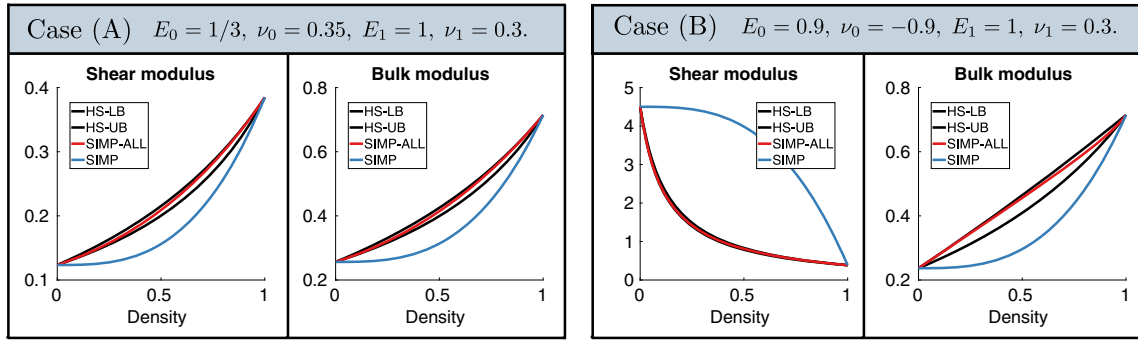


FIGURE 3 Interpolation function comparison when interpolating two real materials. SIMP adaptive interpolation is not even defined. In contrast with SIMP, SIMP-ALL remains in between H-S bounds despite both bounds are really close

In the bimaterial problem, the value of the penalization parameter p for the SIMP interpolation function is unclear. In the following, we take a penalization parameter of value $p = 3$. The SIMP adaptive method is even not defined. The corresponding H-S bounds, SIMP, and SIMP-ALL method have been depicted in Figure 3. As expected, in both cases (A and B), SIMP function falls outside H-S bounds. However, although the space between H-S bounds is significantly narrow, the SIMP-ALL interpolation function comes to lie inside them, as stated in Equation (70). Thus, the use of SIMP-ALL interpolation seems as convenient as the SIMP interpolation for $\nu_1 \simeq 1/3$ and more convenient (from the physical point of view) for different values of ν_1 and when solving bimaterial problems.

7.2 | Numerical examples comparison

In order to see the numerical effects of using different kind of interpolation functions, a cantilever beam example has been solved for the sequence of Cases described in Figure 2. The size of the domain is 2×1 with the left side clamped. A distributed vertical force of unit value is applied in a 0.2 centered part of the right side. The domain is equipped with a structured triangular mesh of 20 000 elements from a Cartesian grid by splitting each cell into four triangles. The density function is approximated with \mathbb{P}_1 Lagrangian finite element functions²¹ and the following filter is applied to the density function:

$$\rho_k = \frac{\sum_{i \in S_k} \int_{\Omega} N_i N_j \rho_j}{\sum_{i \in S_k} \int_{\Omega} N_i}, \quad (75)$$

where ρ_k is the density value in element k and S_k is the set of nodes of element k , see the work of Amstutz et al²² for further details. This filter is defined in a discrete sense, in terms of the shape functions. Other filters depending on the distance are also possible.

We consider the compliance as the cost function and the volume (volume target of the stiff material $V = 0.5$) as a constraint of the topology optimization problem. Additionally, we consider the MMA algorithm,²³ widely used in the community, to solve the problem with a stopping criteria tolerance of 10^{-4} and a maximum number of iterations of $n_{\max} = 5000$. The design variable is initialized with stiff material overall the domain ($\rho = 1$).

As depicted in Figure 4, we observe similar optimal topologies regardless the interpolation used when the Poisson ratio of the stiff material is closed to $\nu_1 = 1/3$. Additionally, the number of iterations and the finite-element solver evaluation are also similar. The examples are computed in MATLAB© with a standard PC (3.40 GHz processor in a 64-bit architecture). However, some differences appear when ν_1 becomes smaller. The optimal topologies when using the SIMP interpolation require large number of iterations and finite-element solver evaluations to converge and gray areas appear. This is probably due to a small penalization value appeared in that cases (see Figure 2). In the case of SIMP adaptive, in which the penalization value is rather large, although it seems to be almost free of numerical instabilities, nonstandard topologies appear. Likewise, a significant computational effort in terms of iterations is required to converge. In contrast, the SIMP-ALL interpolation behaves as adequately in terms of optimal topology and computational effort as




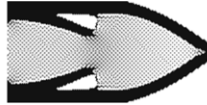
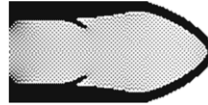










	Case (A) $E_0 = 10^{-3}$ $E_1 = 1$ $\nu_0 = 1/3$ $\nu_1 = 1/3$	Case (B) $E_0 = 10^{-3}$ $E_1 = 1$ $\nu_0 = 1/3$ $\nu_1 = 0$	Case (C) $E_0 = 10^{-3}$ $E_1 = 1$ $\nu_0 = 1/3$ $\nu_1 = -0.5$	Case (D) $E_0 = 10^{-3}$ $E_1 = 1$ $\nu_0 = 1/3$ $\nu_1 = -0.75$	Case (E) $E_0 = 10^{-3}$ $E_1 = 1$ $\nu_0 = 1/3$ $\nu_1 = -0.9$
SIMP interpolation	 $J = 1.592$, $J_{SA} = 1.548$, Iter = 212, FE eval = 214, KKT norm = 8.79×10^{-5}	 $J = 1.616$, $J_{SA} = 1.607$, Iter = 152, FE eval = 154, KKT norm = 9.66×10^{-5}	 $J = 1.694$, $J_{SA} = 1.703$, Iter = 5000, FE eval = 5002, KKT norm = 1.06×10^{-3}	 $J = 1.779$, $J_{SA} = 2.239$, Iter = 4201, FE eval = 4203, KKT norm = 8.30×10^{-4}	 $J = 1.674$, $J_{SA} = 2.988$, Iter = 1870, FE eval = 1872, KKT norm = 8.72×10^{-4}
Adaptive SIMP interpolation	 $J = 1.592$, $J_{SA} = 1.548$, Iter = 212, FE eval = 214, KKT norm = 8.79×10^{-5}	 $J = 1.638$, $J_{SA} = 1.613$, Iter = 219, FE eval = 220, KKT norm = 8.26×10^{-5}	 $J = 1.784$, $J_{SA} = 1.737$, Iter = 116, FE eval = 117, KKT norm = 8.26×10^{-5}	 $J = 2.322$, $J_{SA} = 2.263$, Iter = 393, FE eval = 394, KKT norm = 9.87×10^{-5}	 $J = 2.974$, $J_{SA} = 2.898$, Iter = 1674, FE eval = 1675, KKT norm = 3.90×10^{-5}
SIMP-ALL interpolation	 $J = 1.584$, $J_{SA} = 1.548$, Iter = 108, FE eval = 110, KKT norm = 9.02×10^{-5}	 $J = 1.610$, $J_{SA} = 1.610$, Iter = 164, FE eval = 166, KKT norm = 9.72×10^{-5}	 $J = 1.692$, $J_{SA} = 1.692$, Iter = 211, FE eval = 213, KKT norm = 9.72×10^{-5}	 $J = 1.802$, $J_{SA} = 1.802$, Iter = 142, FE eval = 144, KKT norm = 8.99×10^{-5}	 $J = 1.933$, $J_{SA} = 1.933$, Iter = 170, FE eval = 172, KKT norm = 9.47×10^{-5}

FIGURE 4 Cantilever beam example for a sequence of different material-void interpolations using different interpolation functions. For standard isotropic materials ($\nu_1 = 1/3$), all interpolations behave similarly. As ν_1 becomes more negative, gray areas appear when using SIMP and a larger number of convergence iterations are needed. Adaptive SIMP presents no large gray areas but a noncompetitive cost function and a larger number of convergence iterations appear. SIMP-ALL interpolation presents no gray areas, the number of iterations remains small, and the objective function achieves considerable smaller values. In comparison with SIMP, the SIMP-ALL method evidences an auto-penalizing effect in a wider range of cases [Colour figure can be viewed at wileyonlinelibrary.com]

when considering standard Poisson ratio values, typically $\nu = 1/3$. In Case (C), the SIMP method did not converge. Note that, comparing cost values between interpolation could be fuzzy, since in gray areas, each interpolation proposes different stiffness values. In some cases, SIMP interpolation may propose values stiffer than physically possible (out of H-S bounds). To have a stiffness comparison with physical sense, the cost of the optimal topologies obtained by the three interpolations have been evaluated using the SIMP-ALL interpolation (J_{SA}). The value of the cost (compliance) shown in Figure 4 is normalized with the value of the cost in the initial guess. Admittedly, using the SIMP-ALL interpolation, a decrease in the cost in Case (E) of 35% is obtained when comparing with the SIMP interpolation and of 30% when comparing with the SIMP adaptive interpolation. This result shows the convenience of using the SIMP-ALL interpolation when extreme isotropic materials (see, for example, the work of Greaves et al²⁴) or bimaterial problems are considered.

Finally, the gray areas appearing in the SIMP method is probably because intermediate values with this interpolation are competitive, as seen in Figure 2. Large stiffness values (more than physically possible) are provided for intermediate values. In this case, SIMP behaves not as an auto-penalizing interpolation function. In contrast, SIMP-ALL seems to be auto-penalizing in all the cases. This is not thoroughly surprising since, as shown in Equation (43), the topological derivative (used in the SIMP-ALL interpolation) proposes in fact to insert H-S microstructures near the extreme values. Thus, the possibility of adding a certain amount of density (or inserting certain stiffer inclusions) is not competitive since they provide small stiffness increment. Intuitively, microstructure made of weak material with a small number of circular inclusion transmits barely the load, making it, in general, not attractive from the optimization point of view. This may explain why the proposed SIMP-ALL interpolation, in contrast with SIMP, evidences in the results of Figure 4 an auto-penalizing behavior for all the studied cases.

8 | CONCLUSIONS

The main contributions of this work can be summarized in the following four points.

First, we have showed in Equation (43) that the topological derivative of the compliance is precisely the linear approximation of the H-S bound (lower bound for the weak and upper bound for stiff material). In other words, using the topological derivative for the compliance is equivalent to inserting H-S bound microstructures (circular inclusions). This result strongly relates both concepts and allow us to give a new interpretation of the topological derivative.

Second, we have proposed the SIMP-ALL method, a new interpolation function for the shear and bulk modulus. It is defined as a rational function and build so that its derivative coincides with the H-S lower bound derivative in the weak material and the H-S upper bound derivative in the stiff material, making the gradient coincide, as shown in (43), with the topological derivative in the stiff and the weak material. The key point of the SIMP-ALL interpolation is that in Equation (70), we have shown that it stays always in between the H-S bound regardless the materials to be interpolated, allowing us to interpret its intermediate values always as real microstructures.

Third, we have compared the SIMP-ALL with the SIMP and SIMP adaptive interpolation function. We have observed similar behavior when ν_1 is closed to 1/3 and quite different behavior as it becomes smaller. In contrast with SIMP, the SIMP-ALL interpolation has shown to stay in between the H-S bounds, numerically verifying the result of Equation (70), not only in the case of weak-stiff material but also in the more challenging case of interpolating two general isotropic materials.

Finally, concerning numerical examples, we observed also similar behavior of the optimal topologies around $\nu = 1/3$. However, as it becomes smaller, the SIMP-ALL method has shown to obtain up to 20% stiffer topologies, free of gray areas and smaller computational cost. In comparison with SIMP, this result shows that the SIMP-ALL method is auto-penalizing in a wider range of cases.

From the author's point of view, rather than an alternative, the SIMP-ALL interpolation method can be understood as a generalization of the SIMP method, adequate for all kind of interpolation materials, with physical meaning, free of heuristic parameters, and with no extra computational effort. In this sense, SIMP-ALL interpolation bridge also the gap between the topological derivative community and the SIMP community, allowing the first to use regularized algorithms and the second to use the topological derivative concept. A MATLAB implementation of the SIMP-ALL interpolation is available at <https://github.com/FerrerFerreAlex/SimpALL> and has been also provided in the Appendix.

ACKNOWLEDGEMENTS

The research leading to these results has received funding from the European Union's Horizon 2020 research and innovation programme under the Marie Skłodowska-Curie grant agreement no. 712949 (TECNIOspring PLUS) and from the Agency for Business Competitiveness of the Government of Catalonia. We thank Dr Samuel Amstutz for assistance with developing the methodology, for helping on deeply understand the topic and for the comments that greatly improved the manuscript.

ORCID

A. Ferrer  <https://orcid.org/0000-0003-1011-0230>

REFERENCES

1. Pedersen CBW, Allinger P. Industrial implementation and applications of topology optimization and future needs. In: Bendsoe MP, Olhoff N, Sigmund O, eds. *IUTAM Symposium on Topological Design Optimization of Structures, Machines and Materials*. Dordrecht, The Netherlands: Springer; 2006:229-238.
2. Bendsoe MP, Sigmund O. Material interpolation schemes in topology optimization. *Arch Appl Mech*. 1999;69(9):635-654. <https://doi.org/10.1007/s004190050248>
3. Wang F, Lazarov BS, Sigmund O. On projection methods, convergence and robust formulations in topology optimization. *Struct Multidiscip Optim*. 2011;43(6):767-784. <https://doi.org/10.1007/s00158-010-0602-y>
4. Stolpe M, Svanberg K. An alternative interpolation scheme for minimum compliance topology optimization. *Struct Multidiscip Optim*. 2001;22:116-124.

5. Dzierżanowski G. On the comparison of material interpolation schemes and optimal composite properties in plane shape optimization. *Struct Multidiscip Optim.* 2012;46:693-710.
6. Allaire G, Jouve F, Toader A-M. Structural optimization using sensitivity analysis and a level-set method. *J Comput Phys.* 2004;194(1):363-393. <http://www.sciencedirect.com/science/article/pii/S002199910300487X>
7. Amstutz S, Andrä H. A new algorithm for topology optimization using a level-set method. *J Comput Phys.* 2006;216(2):573-588. <http://www.sciencedirect.com/science/article/pii/S0021999105005656>
8. Allaire G, De Gournay F, Jouve F, Toader AM. Structural optimization using topological and shape sensitivity via a level set method. *Control Cybern.* 2005;34(1):59.
9. Yamada T, Izui K, Nishiwaki S, Takezawa A. A topology optimization method based on the level set method incorporating a fictitious interface energy. *Comput Methods Appl Mech Eng.* 2010;199(45-48):2876-2891.
10. Huang X, Xie YM. A new look at ESO and BESO optimization methods. *Struct Multidiscip Optim.* 2008;35(1):89-92.
11. Baiges J, Martínez-Frutos J, Herrero-Pérez D, Otero F, Ferrer A. Large-scale stochastic topology optimization using adaptive mesh refinement and coarsening through a two-level parallelization scheme. *Comput Methods Appl Mech Eng.* 2019;343:186-206.
12. Nguyen-Xuan H. A polytree-based adaptive polygonal finite element method for topology optimization. *Int J Numer Methods Eng.* 2017;110(10):972-1000.
13. Amstutz S. Connections between topological sensitivity analysis and material interpolation schemes in topology optimization. *Struct Multidiscip Optim.* 2011;43(6):755-765.
14. Sá LFN, Amigo RCR, Novotny AA, Silva ECN. Topological derivatives applied to fluid flow channel design optimization problems. *Struct Multidiscip Optim.* 2016;54(2):249-264.
15. Brezis H. *Functional Analysis, Sobolev Spaces and Partial Differential Equations.* New York, NY: Springer Science; 2010.
16. Novotny AA, Sokolowski J. *Topological Derivatives in Shape Optimization.* Berlin, Germany: Springer-Verlag; 2013. *Interaction of Mechanics and Mathematics Series.*
17. Giusti SM, Ferrer A, Oliver J. Topological sensitivity analysis in heterogeneous anisotropic elasticity problem. Theoretical and computational aspects. *Comput Methods Appl Mech Eng.* 2016;311:134-150.
18. Hashin Z, Shtrikman S. A variational approach to the theory of the elastic behaviour of multiphase materials. *J Mech Phys Solids.* 1963;11(2):127-140.
19. Bendsoe MP, Sigmund O. *Topology optimization: Theory Methods and Applications.* Berlin, Germany: Springer-Verlag; 2003.
20. Allaire G. *Shape Optimization by the Homogenization Method.* New York, NY: Springer-Verlag; 2002. *Applied Mathematical Sciences;* vol. 146.
21. Ern A, Guermond J-L. *Theory and Practice of Finite Elements.* Vol. 159. New York, NY: Springer Science Business Media; 2013.
22. Amstutz S, Dapogny C, Ferrer A. A consistent relaxation of optimal design problems for coupling shape and topological derivatives. *Numerische Mathematik.* 2018;140(1):35-94. <https://doi.org/10.1007/s00211-018-0964-4>
23. Svanberg K. The method of moving asymptotes—a new method for structural optimization. *Int J Numer Methods Eng.* 1987;24(2):359-373.
24. Greaves GN, Greer AL, Lakes RS, Rouxel T. Poisson's ratio and modern materials. *Nature Materials.* 2011;10(11):823.

How to cite this article: Ferrer A. SIMP-ALL: A generalized SIMP method based on the topological derivative concept. *Int J Numer Methods Eng.* 2019;120:361–381. <https://doi.org/10.1002/nme.6140>

APPENDIX

SIMP-ALL MATLAB CODE

In this Appendix, we provide a simplified MATLAB code to facilitate the use of the SIMP-ALL interpolation to the reader. The code is also available at <https://github.com/FerrerFerreAlex/SimpALL>. The *SIMP_all_interpolation.m* function is devised to be used when starting the topology optimization code. The time of computing the interpolation function is negligible making it as usable as the well-established interpolation functions. The constitutive interpolated tensor and its derivative are provided since these are usually used when computing the compliance function and the gradient of the compliance. To obtain the interpolation function, we first compute the shear and bulk modulus and the additional η parameters. Then, the coefficients and the rational function are computed. Finally, we differentiate with respect to the density variable to obtain the derivative.

```

1 function [C,dC] = simp_all_interpolation (E1,E0,nu1,nu0)
2 % SIMP-ALL interpolation function by Alex Ferrer , March 2019.
3 %
4 % E0, nu0 : Young modulus and Poisson ratio of the isotropic weak material
5 % E1, nu1 : Young modulus and Poisson ratio of the isotropic strong material
6 %
7 % C(rho): Isotropic constitutive tensor interpolated from the isotropic
8 % material properties of the strong (E1,nu1) and the weak material (E0,nu0)
9 % through the "density function" rho .
10 %
11 % dC(rho): Derivative of the isotropic material constitutive tensor respect
12 % to the density function rho .
13 %
14 % Remark 1: No conditions are required to E1,E0,nu1,nu0 (except E>0 and
15 % -1<nu < 0.5) , so we could have referred to the strong and weak material as
16 % material A and B. However, we prefer to name them strong and weak to
17 % follow topology optimization naming .
18 %
19 % Remark 2: This version of the SIMP-ALL interpolation function is intended
20 % for 2D plane stress problems .
21 %
22 % Remark 3: SIMP-ALL interpolation evidenced to fulfill the Hashin-Strikman
23 % (HS) bounds for all possible combination of the material properties .
24 % Thus, when the density function takes intermediate values , the resulting
25 % constitutive tensor can be interpreted as an homogenized constitutive
26 % tensor of a micro-structure made of the strong and weak material with a
27 % relative fraction volume of the intermediate density value .
28 %
29 % Remark 4: SIMP-ALL interpolation is free of penalization and heuristic
30 % parameters .
31 %
32 % Remark 5: The interpolation is built on the one hand such that the
33 % constitutive tensor coincides with C0 (constitutive tensor with E0,nu0
34 % material properties ) in rho=0 and with C1 (respectively E1,nu1) in rho=1
35 % and on the other hand such that the constitutive tensor derivative in
36 % rho=0 and rho=1 coincides with the topological derivative of the
37 % compliance dC0 and dC1, i.e.,
38 %          C(0) = C0,          C(1) = C1,
39 %          dC(0) = dC0,        dC(1) = dC1.
40 %
41 % Remark 6: We opt for providing dC since when using the compliance
42 % (integral f*u = integral e(u):C(rho):e(u)) in a topology optimization
43 % problem , its gradient is directly obtained as -e(u):dC(rho):e(u).
44 %
45 % Shear and bulk modulus
46 mu = @(E, nu) E/(2 *(1+ nu));
47 kappa = @(E, nu) E/(2 *(1- nu));
48 %
49 mu0 = mu(E0, nu0);
50 mu1 = mu(E1, nu1);
51 %
52 kappa0 = kappa (E0, nu0);
53 kappa1 = kappa (E1, nu1);
54 %
55 % Auxiliar material property
56 eta_mu = @(mu, kappa )( kappa *mu)/(2 *mu+kappa );
57 eta_kappa = @(mu, kappa ) mu;
58 %
59 eta_mu0 = eta_mu (mu0, kappa0 );
60 eta_mu1 = eta_mu (mu1, kappa1 );
61 %
62 eta_kappa0 = eta_kappa (mu0, kappa0 );
63 eta_kappa1 = eta_kappa (mu1, kappa1 );
64 %
65 % Isotropic fourth order tensor in Voigt notation

```

```

66 I1 = eye(3); I1(3,3) = 1/2;
67 I2 = [1 1 0; 1 1 0; 0 0 0];
68 Aiso = @(alpha , beta ) alpha *I1 + beta *I2;
69 %
70 % Coeficients (n= numerator , d = denominator ) of the rational function
71 n01 = @(f0 , f1 , eta0 , eta1 ) -(f1 - f0)*(eta1 - eta0 );
72 n0 = @(f0 , f1 , eta0 ) f0*(f1 + eta0 );
73 n1 = @(f0 , f1 , eta1 ) f1*(f0 + eta1 );
74 d0 = @(f1 , eta0 ) (f1 + eta0 );
75 d1 = @(f0 , eta1 ) (f0 + eta1 );
76 %
77 n01_mu = n01(mu0 , mu1 , eta_mu0 , eta_mu1 );
78 n01_kappa = n01(kappa0 , kappa1 , eta_kappa0 , eta_kappa1 );
79 %
80 n0_mu = n0(mu0 , mu1 , eta_mu0 );
81 n0_kappa = n0(kappa0 , kappa1 , eta_kappa0 );
82 %
83 n1_mu = n1(mu0 , mu1 , eta_mu1 );
84 n1_kappa = n1(kappa0 , kappa1 , eta_kappa1 );
85 %
86 d0_mu = d0(mu1 , eta_mu0 );
87 d0_kappa = d0(kappa1 , eta_kappa0 );
88 %
89 d1_mu = d1(mu0 , eta_mu1 );
90 d1_kappa = d1(kappa0 , eta_kappa1 );
91 %
92 % Density function (symbolic in order for further differentiation)
93 rho = sym( 'rho ' , 'positive ' );
94 %
95 % SIMP-ALL as a rational function
96 f = @(n01 , n0 , n1 , d0 , d1 , rho ) ...
97 (n01*(1-rho)*(rho) + n0*(1-rho) + n1*rho)/(d0*(1-rho)+d1*rho);
98 %
99 mu = f(n01_mu , n0_mu , n1_mu , d0_mu , d1_mu , rho );
100 kappa = f(n01_kappa , n0_kappa , n1_kappa , d0_kappa , d1_kappa , rho );
101 %
102 % Isotropic constitutive tensor .
103 Csym = simplify ( Aiso (2*mu , kappa - mu) );
104 %
105 % Shear and bulk modulus derivatives
106 dmu = diff (mu);
107 dkappa = diff (kappa );
108 %
109 % Isotropic constitutive tensor derivative
110 dCsym = Aiso (2*dmu , dkappa-dmu);
111 %
112 % In order to obtain a handle function instead of a symbolic expression and
113 % to directly evaluate the constitutive tensor (and derivative ) for any
114 % vector of densities , we make use of matlabFunction ( ) .
115 nstre = 3; % Number of stress components in Voigt notation in plane stress
116 dC = cell(nstre , nstre );
117 for i=1:nstre
118     for j=1:nstre
119         if Csym(i , j)==0
120             C{i , j} = @(rho ) zeros (size (rho ));
121             dC{i , j} = @(rho ) zeros (size (rho ));
122         else
123             C{i , j} = matlabFunction (Csym (i , j));
124             dC{i , j} = matlabFunction (dCsym (i , j));
125         end
126     end
127 end
128 end

```

In the following, we present an example for using the interpolation function in a common finite element context.

```

1 function Use_example_of_simp_all_interpolation
2 % Use example of the SIMP-ALL interpolation function for computing the
3 % compliance and its gradient , by Alex Ferrer , May 2018.
4 %
5 % From a given material isotropic properties values
6 E1 = 1;
7 E0 = 0.01;
8 nu1 = 1/3;
9 nu0 = 1/3;
10 % Build the SIMP-ALL interpolation of the constitutive tensor as
11 [C,dC] = simp_all_interpolation (E1,E0,nu1,nu0);
12 %
13 %In the context of a FE problem , for a given number of gauss points nkaus
14 % and number of elements nelelem of for example
15 nelelem = 1000;
16 nkaus = 4;
17 %
18 % and for a given a density values 0 <= rho <= 1 of dimension
19 % dim(rho) = nkaus x nelelem of for example
20 rho = rand (nkaus ,nelelem );
21 %
22 % and for a given strain tensor values in Voigt notation (nstres = 3)
23 % obtained from the solution of a finite element problem KU=F of for example
24 nstres = 3;
25 strain = rand (nstres ,nkaus ,nelelem );
26 %
27 %Although it would be cheaper with F*U, defining dV (weight*Jacobian )
28 dV = rand (nkaus ,nelelem );
29 %the compliance can be computed as
30 c = 0;
31 for istres = 1:nstres
32     for jstres = 1:nstres
33         str = squeeze ( strain (jstres ,:,:) );
34         aux = str .* C{istres ,jstres }(rho) .* str .* dV;
35         c = c + sum (aux (:));
36     end
37 end
38 %
39 % and the gradient of the compliance as
40 g = zeros (nkaus ,nelelem );
41 for istres = 1:nstres
42     for jstres = 1:nstres
43         str = squeeze ( strain (jstres ,:,:) );
44         g = g - str .* dC{istres ,jstres }(rho) .* str ;
45     end
46 end
47 end

```